https://doi.org/10.15407/ufm.25.02.386

M.A. LATYPOVA [1,*] and A.T. TURDALIEV [2]

[1] Karaganda Industrial University,
Republic Ave. 30, 101400 Temirtau, Kazakhstan

[2] M. Auezov South Kazakhstan University,
Tauke Khan Avenue, 5,
160012 Shymkent, Kazakhstan

* m.latypova@tttu.edu.kz

ADDITIVE TECHNOLOGIES FOR 3*D* PRINTING WITH METALS

Additive 3*D* printing technologies dynamically developing at a rapid pace are used in progressive industries. There are several types of additive technologies based on different physical principles: selective laser melting (SLM), electron beam melting (EBM), fused deposition modelling (FDM), lamination object manufacturing (LOM), *etc*. They are all united by one technological principle — the production of items through layer-by-layer construction. Similar to traditional shaping methods, each type of additive technology has advantages and disadvantages. The principal materials traditionally used for functional products of various purposes are metals and alloys. Two main technologies for fabrication of metal products are currently well developed worldwide: SLM and EBM. Despite the high accuracy and decent quality of the products obtained by means of these technologies, they have several disadvantages, including the high cost of both the technological equipment and the raw materials used.

Keywords: selective laser melting, additive technologies, microstructure, microstructure control, heat treatment.

1. Introduction

Additive technologies (AT) are one of the breakthrough directions in modern science and technology development. These technologies are based on the scientific aspects of the behaviour of materials during their high-energy processing. It is possible to obtain the specified properties of the material using additive technologies by applying knowledge of materials

Citation: M.A. Latypova and A.T. Turdaliev, Additive Technologies for 3*D* Printing with Metals, *Progress in Physics of Metals*, **25**, No. 2: 386–415 (2024)

science and understanding what structure will be formed in the finished product [1–10].

Now, almost every home, office, and enterprise has available 3*D* printing technologies in the form of installations implementing the FDM method. These installations have the main advantages — their low price and ease of use, the ability to easily control the obtaining process, sufficiently high production accuracy, and speed of construction. The already traditional technology of injection moulding polymer-powder mixtures into metal moulds also uses one of the principles and advantages of additive manufacturing — product formation by addition. Powder injection moulding (PIM) technology has been used in the high-precision production of metal products (MIM — injection moulding with metals) of complex configurations since the 70s of the XX century and is a continuation of the development of powder metallurgical technologies. The main disadvantages of using this technology are the need to use complex technological equipment, expensive tooling for casting a 'green' part, and the inability to obtain parts with a complex internal structure. FDM technology also uses polymer raw materials to produce complex-shaped products using 3*D* printing. At the same time, the PIM starting materials, which are a polymer highly filled with metal powder, are affordable in terms of price and technology for obtaining raw materials.

The essence of AT consists of the layered construction of products, models, forms, and master models by fixing layers of model material and their sequential connection to each other in various ways: sintering, fusion, gluing, and polymerization — depending on the nuances of a particular technology. In other words, additive technologies involve a part formation by sequentially 'building up' the material layer-by-layer [11–18].

The precursors of modern AT are considered two original technologies that appeared in the XIX century. In 1890, Josef E. Blanther proposed a method for making topographic layouts – three-dimensional maps of the terrain surface. The essence of the method was as follows: fragments corresponding to an imaginary horizontal section of the object were cut out of thin wax plates along the contour lines of a topographic map, and then these plates were stacked one on top of another in exact order and glued together. The result was a 'layered synthesis' of a hill or ravine. After that, the paper was applied on top of the obtained figures, and a layout of a separate landscape element was formed, which was then placed in paper form following the original map. This idea has found practical application in LOM technology — layered lamination (lamination object manufacturing) or gluing of thin sheet materials, the thickness of the sheets is 0.051–0.25 mm.

In 1979, Professor Nakagawa from the University of Tokyo proposed using this technology for the rapid manufacture of moulds, in particular, with the complex geometry of cooling channels.

The second technology, photo sculpture, was proposed by Frenchman Franзois Willиme in 1890. Its essence was as follows: cameras were placed around the object or subject, and simultaneous photographing was performed on all cameras. Then each image was projected onto a translucent screen, and the operator used a pantograph to outline the outline. The pantograph was connected to a cutting tool that removed the model material, clay, according to the profile of the current contour.

To reduce the complexity of this process, the German Carlo Baese in 1904 proposed photosensitive gelatine use, which expands when treated with water depending on the degree of exposure.

In 1935, Isao Morioka proposed a method combining topography and photo sculpture. The method involved structured light use (a combination of black and white stripes) to create a topographic 'map' of the object — a set of contours. The contours were then cut out of sheet material and laid in exact order to form a three-dimensional image of the object.

In 1977, Wyn Kelly Swainson proposed a method for producing three-dimensional objects by curing a photosensitive polymer at the intersection of two laser beams. At about the same time, technologies for layer-by-layer synthesis from powder materials began to appear (P.A. Ciraud, 1972).

In 1981, R.F. Housholder proposed a method for forming a thin layer of powder material by applying it to a flat platform. Next, levelling was performed to a certain height with subsequent layer sintering. In the same year, Hideo Kodama published the results of work with the first functional photopolymerization systems using an ultraviolet lamp and a laser.

The technology of 'three-dimensional printing' appeared in the late 80s of the last century. The founder of the industry was Charles W. Hull, the founder of the company that was the first to start commercial activities in the field of layered synthesis. In 1986, Charles W. Hull proposed a method for layered synthesis using ultraviolet radiation focused on a thin layer of photopolymer resin. He also coined the term 'stereolithography'. In the same year, the engineer assembled the world's first stereolithographic 3*D* printer — stereolithographic apparatus (SLA), thanks to which digital technologies have made a vast leap forward. Around the same time, Scott Crump released the world's first FDM device. Since then, the three-dimensional printing market has been growing rapidly and replenished with new models of unique printing equipment.

Until the mid-90s, they were mainly used in research and development activities related to the defence industry. The first laser machines, first stereolithographic (SLA machines), then powder (SLS machines), were overpriced, and the choice of model materials was very modest. However, in 1995, a turning point was ripe, which made additive manufacturing methods generally available. Students of the Massachusetts Institute of Technology, Jim Bredt, and Tim Anderson, have implemented the technology of layer-by-layer synthesis of material into the body of a conventional

desktop printer. That is how Z Corp. was founded, which has long been considered a leader in the field of household printing of three-dimensional figures.

The widespread use of digital technologies in the field of design (CAD), modelling and calculations (CAE), and machining (CAM) has stimulated the explosive nature of the development of 3*D* printing technologies, and now, it is challenging to specify an area of material production where 3*D* printers would not be used to one degree or another [1].

2. Selective Laser Melting

Selective laser melting is one of the new additive methods that appeared in the late 1980s and 1990s [4]. During the SLM process, the product is formed by selectively melting successive powder layers by laser beam interaction. After irradiation, the powder material heats up and, with sufficient power, melts and forms a liquid pool. After that, the molten pool solidifies and cools quickly, and the consolidated material begins to form the product. After the section of the layer is scanned, the construction platform is lowered by an amount equal to the thickness of the layer, and a new layer of powder is applied. This process is repeated until the product is completed [19]. The non-irradiated material remains in the construction cylinder and is used to support subsequent layers.

Compared to conventional manufacturing technologies, SLM offers a wide range of advantages, namely lower time to market, production of almost pure moulds without the need for expensive moulds, high material utilization rate, direct production based on the CAD model, and a high level of flexibility. In addition, due to additive and layered products, the SLM process can create complex geometric features that cannot be obtained using conventional production routes [19].

Unfortunately, this new production technology deals with some frequently observed problems. SLM is characterized by high-temperature gradients, which leads to an increase in thermal stresses and rapid solidification, which leads to the occurrence of segregation phenomena and the presence of nonequilibrium phases [19].

However, the manufacture of metal products through SLM has many difficulties. High input heat often causes an increase in evaporation and splashing of the material during processing. Figure 1 shows the laser scanning strategy for making three-dimensional models. One scan cycle looks like this: 1 — scanning only the contour; 2 — scanning the contour and hatching inside 3 — scanning only the fragment 4 — scanning the contour and hatching inside in the X direction [6].

Density after SLM is the first and perhaps the most essential problem in this process since density determines the mechanical properties of the part, which, in turn, has a direct impact on the performance of the com-

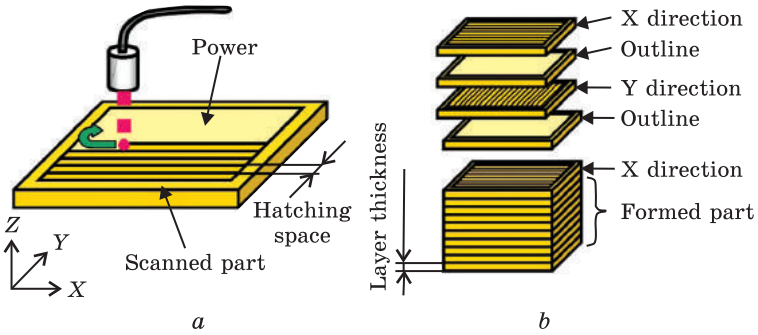

Fig. 1. An example of a laser beam scanning when creating a three-dimensional model: *a* — hatching in the X direction, and *b* — the direction of hatching [2]

ponent [8, 9]. The goal in SLM is often to get 100% dense parts. However, this goal is hard to achieve because there is no mechanical pressure, as in moulding processes, only temperature effects, gravity, and capillary forces characterize SLM during SLM. In addition, gas bubbles can enter the material during solidification caused by various reasons [20, 21]. Porosity is still a problem, even for conventional processes such as injection moulding [14, 22].

SLM technology has many advantages, but there are considerable disadvantages, such as a large amount of powder being wasted and a high installation cost.

3. Electron Beam Melting

Electron beam melting is an additive complete melting process that relies on metal powder and high beam energy [23, 24]. EBM is one of the few additive technologies that can realize the production of fully functional high-density parts, especially concerning complex parts with high quality [25, 26].

The EBM process is functional to work with many different classes of materials, such as stainless steel, tool steel, nickel heat-resistant alloys, low coefficient of expansion alloys (Invar), heavy metals (NiWC), intermetallic compounds, aluminium, copper, beryllium and niobium [26]. However, the use of this technology is currently focused on titanium and various titanium alloys [26, 27]. Typical titanium is traditionally made by forging [28, 29], pressing [29], or casting [30, 31].

One of the problems of this technology concerns complex geometries, which are expensive to make using conventional technological processes [26]. EBM technology is more suitable for these materials [26, 27] while working in a vacuum environment and with high power, and their use is becoming more common [32, 33]. Applications are now found in medical implants

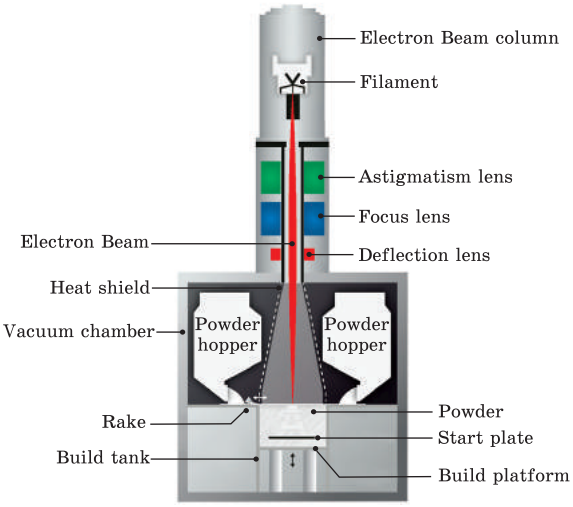

Fig. 2. Components of the Arcam machine [107]

[34, 35], as well as automotive [36, 37] and space parts [38, 42]. The use of the EBM process in the medical field allows the patient to manufacture individual implants with a complex structure and shape, which show high biocompatibility and osseointegration [34, 35, 38].

One of the successful examples is the mass production of titanium acetabular cups and turbine blades, turbochargers, wheels, and valves for internal combustion engines [39–45].

The aerospace industry currently uses the advantages of high-performance, lightweight, and complex products [26, 46]. In this area, the EBM process allows you to reduce the time to merchandise and reduce the cost of development. That is due to a decrease in the number of production steps and a decrease in material waste [26] since powders can be recycled several times without any noticeable changes in their chemical composition or physical properties [26, 67]. Special attention is paid to the production of high-density products made of Ti–Al alloys, as these materials have shown interesting properties for use in the aerospace industry, such as low density, high specific strength, high specific stiffness, crack resistance [34, 48–51], ductility, fatigue strength, creep [26, 52], corrosion resistance and oxidation at high temperatures [36, 41, 53].

As for the technologies used to create an electron beam, the EBM system is similar to a welding machine, and the principle of operation is similar to an electron microscope. The Arcam Company, which was founded in 1997, developed the first electron beam installation for additive manufacturing of products [22]. Figure 2 shows the main components of the Arcam machine: an electron beam cannon and a platform for building apart. The electron beam cannon consist of an upper column containing an electron-generating part and a lower column containing magnetic lenses used to form and deflect the beam. The heated cathode filament emits electrons in the upper column. The potential between the cathode and the anode is usually about 60 kV. Electrons are accelerated to a speed in the range from 0.1 to 0.4 of the speed of light [54]. A magnetic lens [24] controls the shapes and deviations of the electron beam. The first set of coils (astigmatic lenses) adjusts the shape of the beam, and the second set of

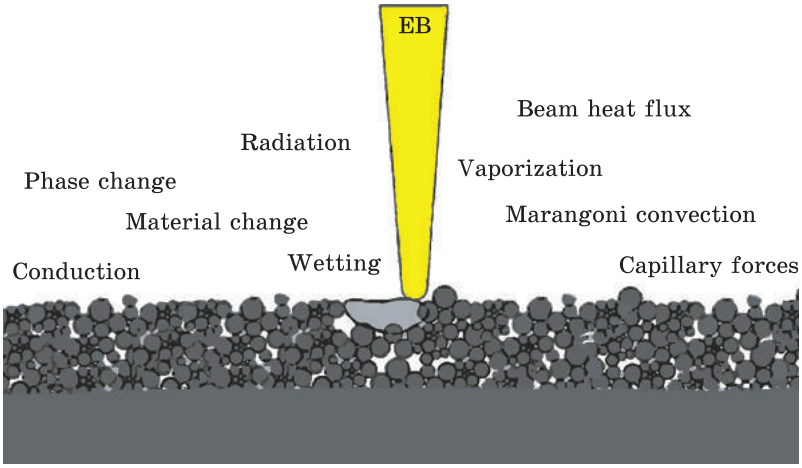

Fig. 3. The processes occurring during EBM [107]

coils (focus lenses) adjusts the size of the beam. The last set of coils is used to focus the beam onto the construction platform [49], according to a given geometry. The electron gun is fixed, so there is no mechanical part that is used to control or deflect the beam. The whole process takes place in a vacuum to avoid scattering electrons from the air molecules. The vacuum is created using turbomolecular pumps. The working pressure in the processing chamber is usually about 10^{-3} Pa [26]. During the melting process, a small amount of inert helium gas is added to avoid the accumulation of electric charges in the powder, as well as to ensure the thermal stability of the process [55].

The scanning power and speed are reduced for subsequent fusion steps. After the selective melting phase, the construction platform is lowered by one layer of thickness, and a new layer of powder from the bins is applied with a squeegee. The process is repeated until the product is completed. After construction, the part remains until it cools completely under increased helium pressure. At the end of the process, when the part is removed from the chamber, the soft agglomerate of the powder remains baked on the finished parts and covers them completely [28, 49]. This agglomerate is called powder waste [55], and it is removed by sandblasting using the initial powder of the material [38]. Since there is not even a minimum amount of oxygen in the chamber [53], leftover powder can be used several times with no change in its chemical composition or physical properties.

The EBM process involves several physical mechanisms, as shown in Fig. 3. These mechanisms are complex because the scanning speed is very high, and phase changes occur within a very short time [56]. The key mechanism is the interaction between electrons and powder. When elec-

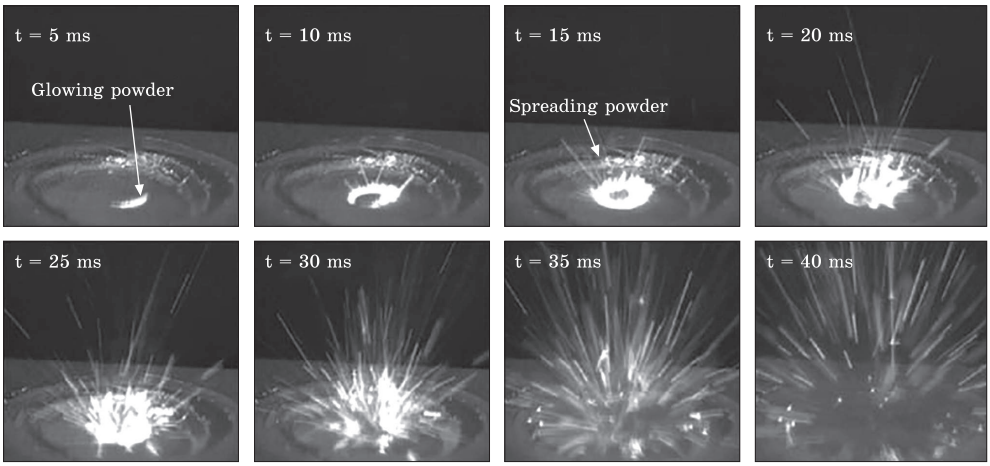

Fig. 4. Applying a layer of powder without heating (preliminary) [25]

trons collide with powder particles, most of their kinetic energy is released in the form of thermal energy, which melts, sinters, heat, and vaporizes the material [56]. The remaining kinetic energy is converted into radiation and secondary electrons that leave the surface.

The interaction between the electron beam and the powder involves four main consequences: particle scattering, particle sintering, particle melting, and evaporation of some alloying elements.

The scattering of powder particles occurs as an explosion, as shown in Fig. 4 [23]. This spread can be generated by (i) residues of water or moisture in the powder, which can evaporate by the explosion, (ii) an impulse transmitted to electrons, which are greater than cohesive interactions in the powder, and (iii) a negative electrostatic charge of the powder particles, which causes mutual repulsion between the particles [24, 57].

The advantages of this technology include high accuracy, which is achieved using 'magnetic mirrors' that correct the trajectory of the electron beam. SLS technology uses optical mirrors that have lower positioning accuracy. Laser mirrors and lenses are expensive. Depending on the installation power, mirrors can have a gold or silver coating, and lenses can be either diamond or germanium. Low-cost materials are used in EBM for the production of electromagnetic components. If necessary, the electron beam can be scattered, which makes it possible to heat the source material without additional elements that are necessary for laser installations. The absence of complex mechanical components makes it possible to achieve a higher beam movement speed, which, together with an increase in its energy, allows for higher productivity. Another advantage is the ability to produce several products at once without additional heat treatment.

The main disadvantages of the process include the presence of x-ray radiation, which occurs when electrons bombard metals; therefore, an absorbing coating must be installed in the working chamber. In addition, now, electron beam melting is limited to an accuracy of 0.2 mm, due to the size of the electron beam, which is of 0.2–1.0 mm, which leads to a slight roughness of the finished products. The main disadvantage is that today there is no full-fledged home 3*D* printer; this method is available only on an industrial scale [23].

4. Direct Method of Laser Sintering

The direct method of laser sintering (DMLS) is a method of direct laser sintering, a technology for additive manufacturing of metal products developed by EOS from Munich. DMLS is often confused with a similar selective laser melting technology [58].

The process involves using three-dimensional models in STL format as drawings to build physical models. The three-dimensional model is digitally processed for virtual separation into thin layers with a thickness corresponding to the thickness of the layers applied by the printing device. The finished 'building' file is used as a set of drawings during printing. Fibre-optic lasers of relatively high power (of about 200 W) are used as a heating element for sintering metal powder. Some devices use more powerful lasers with increased scanning speed (*i.e.*, movement of the laser beam) for higher performance. Alternatively, it is possible to increase productivity by using multiple lasers. DMLS allows you to create solid metal parts of complex geometric shapes [59].

The powder material is fed into the working chamber in the quantities required for applying a single layer. A special roller aligns the supplied material into an even layer and removes excess material from the chamber, after which the laser head sinters the particles of fresh powder between each other and with the previous layer according to the contours defined by the digital model. After the drawing of the layer is completed, the process is repeated: the roller supplies fresh material and the laser begins to sinter the next layer. An attractive feature of this technology is the very high print resolution of about 20 microns on average. For comparison, the typical layer thickness in amateur and household printers using FDM technology is of about 100 microns [60–63].

Another captivating feature of the process is the absence of the need to build supports for overhanging structural elements. The non-sintered powder is not removed during printing but remains in the working chamber. Thus, each subsequent layer has a support surface. In addition, unspent material can be collected from the working chamber upon completion of printing and reused. DMLS production can be considered virtually waste-free, which is essential when using expensive materials, *e.g.*, precious metals.

The technology has practically no restrictions on the geometric complexity of construction, and high precision of execution minimizes the need for mechanical processing of printed products.

DMLS technology has several advantages over traditional manufacturing methods. The most obvious is the ability to produce quickly geometrically complex parts without the need for machining. Production is practically waste-free, which distinguishes DMLS from traditional technologies. The technology allows you to create several models at the same time with a limit only on the size of the working camera. Building models take about several hours, which is disproportionately more profitable than the casting process, which can take up to several months, including the complete production cycle. On the other hand, parts produced by laser sintering do not have solidity and, therefore, do not achieve the same strength indicators as cast samples or parts produced by traditional methods.

DMLS is actively used in industry due to the possibility of building internal structures of solid parts that are inaccessible due to the complexity of traditional production methods. Parts with complex geometry can be made wholly rather than from parts, which favourably affects the quality and cost of products. Since DMLS does not require special tools (for example, moulds) and does not produce a large amount of waste, unlike traditional methods, the production of small-scale batches using this technology is much more profitable than using traditional methods.

DMLS technology is used for the production of small and medium-sized finished products in various industries, including aerospace, dental, medical, *etc*. The typical size of the construction area of existing installations is $250 \times 250 \times 250$ mm, although there are no technological restrictions on the size — it is just a matter of the cost of the device. DMLS is used for rapid prototyping, reducing the development time of new products as well as in production, allowing you to reduce the cost of small batches and simplify the assembly of products of complex geometric shapes.

The Northwestern Polytechnic University of China uses DMLS systems to produce aircraft structural elements. Research conducted by EADS also indicates a reduction in cost and waste when using DMLS technology to produce complex structures in single copies or small batches.

5. Metal Injection Moulding

Metal injection moulding (MIM) is a method of manufacturing metal parts. MIM is a subcategory of Powder injection moulding Technology (PIM). PIM uses plastic injection moulding technology with a feedstock consisting of a polymer and an inorganic material. The inorganic component of the raw material can be metal or ceramics. The fundamental idea of the MIM production method is to combine the advantages of injection moulding with the elastic mechanical properties of metals. This approach allows the pro-

duction of complex and detailed metal parts with high strength and rigidity. Traditional casting methods require the metal to be in a molten state during casting metal powder and polymer raw materials used in MIM allow the moulding process to be carried out at much lower temperatures [64].

6. Indirect Metal Laser Sintering

The process called indirect metal laser sintering (IMLS) was developed by DTMcorp of Austin in 1995. Since 2001, DTMcorp has been owned by 3*D*-Systems. During the indirect laser sintering process, a mixture of powder and polymer or polymer-coated powder is used, where the polymer acts as a binder and provides the necessary strength for further heat treatment. At the heat treatment stage, polymer distillation, sintering of the frame and impregnation of the porous frame with a metal bundle are carried out, as a result of which the finished product is obtained. For indirect laser sintering, powders of both metals and ceramics or mixtures thereof can be used. Preparing a mixture of powder and polymer is carried out by mechanical mixing, while the polymer content is about 2–3% (by weight), and in the case of using a polymer-coated powder, the layer thickness on the surface of the particle is about 5 microns. Epoxy resins, liquid glass, polyamides, and other polymers are used as binders. The distillation temperature of the polymer is determined by its melting and decomposition temperature and averages 400–650 °C.

After distillation of the polymer, the porosity of the product before impregnation is about 40%. During impregnation, the furnace is heated 100–200 °C above the melting point of the impregnating material, since with increasing temperature the wetting angle decreases and the viscosity of the melt decreases, which favourably affects the impregnation process. Usually, the impregnation of future products is carried out in an aluminium oxide backfill, which plays the role of a supporting frame, since, during the period from polymer distillation to the formation of strong interparticle contacts, there is a danger of destruction or deformation of the product. Protection against oxidation is organized by creating an inert or reducing medium in the furnace. Quite a variety of metals and alloys can be used for impregnation, which meets the following conditions. The impregnation material should be characterized by a slight interfacial interaction or its complete absence, a small wetting angle, and a melting point lower than that of the substrate. For example, if the components interact with each other, undesirable processes may occur during the impregnation process, such as the formation of more refractory compounds or solid solutions, which may lead to a halt in the impregnation process or negatively affect the properties and dimensions of the product. Usually, bronze is used to impregnate the metal frame, while the shrinkage of the product is 2–5% [65].

7. Selective Thermal Sintering

Selective thermal sintering (SHS) is an additive manufacturing method. The technology is based on melting layers of thermoplastic or metal powder using a thermal emitter. Upon completion of the formation of the layer, the working platform moves down to a distance corresponding to the thickness of one layer, after which a new layer of powder is applied using an automated roller, and then a new layer is sintered along the contours specified by a digital three-dimensional model. SHS technology is best suited for the production of modest functional prototypes. Selective thermal sintering is similar to selective laser sintering (SLS). The only significant difference between these two methods is the use of a thermal print head instead of a laser one. This solution allows you to reduce the cost and dimensions of printing devices, up to the possibility of creating desktop printers. On the other hand, the energy efficiency of SHS devices is low compared to 3*D* laser printers, which significantly limits the choice of materials [66].

One of the main advantages of the thermal sintering method is that for a definite wavelength of IR radiation, it is always possible to select two types of material: one of which will transmit heat, and the other will absorb it. Thus, by combining these materials in the production of a product, it is possible to achieve considerable complexity and a variety of forms. Selective laser sintering is a real breakthrough in high-speed three-dimensional printing. It is important to emphasize that the model is formed from powder, and all unused powder can be reused. This technology allows you to produce models of the most complex geometric shapes as well as allows you to print several parts at the same time. As a rule, thermoplastic polymers or rather low-melting metals are used as consumables. In the latter case, models often require additional firing to increase strength [67].

8. Equipment for 3*D* Metal Printing

Metal powders are the most durable material for 3*D* printing. Products created on metal 3*D* printers are superior in many respects to analogues produced using traditional technologies.

Titan. A high-strength biocompatible material used in medicine, aircraft engineering, mechanical engineering, and industry.

Tool and stainless steel. Various steel alloys are the most common materials for 3*D* printing. They serve to solve a wide range of tasks in different fields, are resistant to corrosion, and have increased strength and wear resistance.

Aluminium and Its Alloys. A lightweight alloy with a lower density than other metals for 3*D* printing. It has good drainage properties and

electrical conductivity. It is used in the automotive industry, aerospace industry, and industry.

Cobalt–Chrome. Corrosion-resistant biocompatible material. It has high strength and is used in medicine and dentistry, as well as in industries with high temperatures.

Nickel Alloys. A material with excellent mechanical strength and weldability. Stable up to 3000 °C. It is used in aviation, energy, tool manufacturing, and other industries.

3*D* printers can be used to print large-format sets of materials. According to the technical specification, the additive machine can be configured.

The plants used in additive manufacturing can be divided into two main categories: layer deposition and direct deposition.

Selective laser melting machines are the most numerous and diverse in terms of the method of creating a group structure. In such installations, a laser is used as an energy source for connecting particles of a metal-powder composition. Such machines include such companies as 3*D* Systems, Concept Laser, EOS, Renishaw, and SLM Solutions.

3*D* printing plants are complex and include devices for sieving and feeding powder material, cleaning machines, cooling and filtration systems, metal powder storage, systems for generating and supplying inert gases, *etc*. Consider the installations of well-known manufacturers.

3*D* Systems (USA) offers six 3*D* printing machines: from the smallest DMP Flex 100, with a $100 \times 100 \times 90$ mm construction camera and a 100 W laser power, to an industrial-scale installation — DMP Factory 500 with a $500 \times 500 \times 500$ mm construction platform and 3 lasers up to 500 W.

The Concept Laser Company has been producing installations for three-dimensional printing since 2007. To date, 5 cars are being produced. The younger model, Mlab cusing R, has three construction platform options: $50 \times 50 \times 80$ mm, $70 \times 70 \times 80$ mm, and $90 \times 90 \times 80$ mm. A laser with a power of 100 W. The older model — X LINE 2000R, has a construction platform with dimensions of $800 \times 400 \times 500$ mm. Two lasers with a power of 1000 W each. The construction of the part is possible in two media: N_2 or Ar.

The British company Renishaw produces only two installations for three-dimensional printing. RenAM 500Q is a multi-laser system that includes four lasers with a power of 500 watts each. The construction volume of this installation is $250 \times 250 \times 350$ mm. Argon is used as an inert gas. The second model is the RenAM 500S. The characteristics are the same as those of the older model, but the only difference is that the laser system has at its disposal only one laser with a power of 500 W. However, this model can be retrofitted with a multibrowser system. Both installations support printing with the following metal powder materials: Ti_6Al_4V titanium alloy, AlSi10Mg Aluminium alloy, CoCr Cobalt Chromium alloy, 316L Stainless Steel, and Nickel alloys.

Another well-known manufacturer of 3*D* printing equipment is the German company EOS, which can offer five installations. The smallest — is EOS M 100, which has a laser with a power of 200 W and a construction site of 100×95 mm, to the largest — is EOS M 400-4, which is a multilaser system with four lasers with a power of 400 W each and having a building volume of 400×400×400 mm.

The developer of Direct Metal Deposition (DMD) technology is POM (precision optical manufacturing), which was acquired by the American company DM3D in December 2012. To date, installations of DM3*D*, Optomec (USA), Sciaky (USA), BeAM (France), and InssTek (South Korea) companies are using this technology [67].

Optomec supplies the 3*D* printing market with metal printers such as LENS MR-7, LENS 450, and LENS 850-R, which are used for the rapid prototyping of titanium, stainless steel, and Inconel parts. LENS systems allow layers to be applied with different materials (they can be equipped with two or more bunkers with different materials), as well as to carry out rapid material change. The printing areas of the 3*D* printers LENS 450, LENS MR-7, and LENS 850-R, respectively, are 100×100×100 mm, 300×300×300 mm, and 900×1500×900 mm.

The commercial implementation of the EasyCLAD (Easy construction laser additive direct) technology, developed by Irepa Laser, is carried out by BeAM, supplying six types of machines with different working area sizes (from 400×250×200 mm for the Mobile model, optimal for working with small and medium-sized parts up to 1200×800×800 for the Beam Magic 2.0 and Magic 800 models used in aerospace industries for the creation and restoration of turbines).

9. Metals Used in 3*D* Printing

3*D* printers can use a wide range of materials for printing. According to the technical specification, the additive machine can be configured to work with almost any other type of metal: tungsten, Ni–Cd alloys, iron, and copper. However, the process of setting up a 3*D* printer for a new material is accompanied by many difficulties and is still possible only experimentally, which does not always allow you to use the full capabilities of the printer.

There are works [66, 67], in which noble metals such as gold and platinum are used as a material; but these works have not received a significant continuation of research.

Several factors contribute to the limited metal palette. When it comes to melting, metals, as a rule, must be weldable and castable to be processed successfully in the three-dimensional printing process. A small, moving melt bath is significantly smaller than the size of the final part (usually about 102–104 times smaller). This local hot zone, which is in direct con-

tact with a large and colder zone, leads to the appearance of large thermal gradients, causing significant thermal residual stresses and nonequilibrium microstructures. For powdered raw materials, the particles should preferably be spherical with a definite size distribution, which differs for PBF and DED. The latter, as a rule, are less sensitive to the dimensional qualities of raw materials. The wire is also a suitable starting material for definite DED processes, creating a larger melt reservoir compared to powder-based DED, which provides higher productivity [68].

Most of these metal powders are typically produced using well-established methods such as spraying in water, gas, or plasma. Low-cost processes are currently being developed or are already being used for the cost-effective production of metal powders, for example, electrolytic methods, metallothermic processes (for example, the TIRO process), and the hydride–dihydride process, especially in the field of titanium and titanium alloys.

Different powder production methods result in various powder characteristics such as particle morphology, particle size, and chemical composition, each of which may be important to AM. In principle, the AM process requires good feeding properties to achieve uniform powder distribution, as well as, good packaging characteristics to form a powder layer with a high relative density. These powder characteristics affect the properties of the bulk material of the manufactured component, for example, its density and porosity.

The most effortless and inexpensive spraying process is spraying in water. In this process, the liquid metal is sprayed by jets of water in free fall through the spray chamber. Due to the high cooling rate, particles ranging in size from several microns to 500 microns take an irregular shape during solidification [69].

The irregular, asymmetric shape of the particles is at a disadvantage with high packing density. Thus, these particle types are not preferred for use in AM [70]. Compared with gas-atomized powders, when sprayed in water, powder particles with higher oxygen content are formed [71]. As for the use of the resulting metal powder in additive manufacturing, oxygen absorption and the formation of oxidants are undesirable effects since they not only affect the powder behaviour but also affect the melt reservoir and, consequently, change the composition of the bulk material and the mechanical properties of parts [72].

10. Modelling of 3*D* Printing Processes

Various software is used for numerical finite element modelling of three-dimensional printing processes: Ansys [73], Adina [74, 75], Abaqus [76], Comsol [77], and Marc [78].

The mechanical properties of materials [79], heat transfer [79, 80], and a melt bath [81] are studied using numerical modelling. The material

deposition in additive manufacturing is modelled using inactive or silent elements that are activated as the added material (powder or wire) solidifies [80]. Two metal deposition methods are used to simulate material deposition: 1) the use of quiet or 2) the use of inactive elements [82, 83]. With the silent approach, the elements are present in the analysis, but they are assigned properties, so they do not affect the analysis. In the inactive element approach, elements are not included in the analysis until the appropriate material is added. In Ref. [80], the application of the finite element method for modelling heat transfer during metal deposition during 3*D* printing is investigated. The author notes that when using general-purpose codes of the finite element method, it is difficult to determine the interface between active and inactive elements in consequence, surface convection, and radiation at this constantly changing interface are often neglected in modelling. The author showed that such neglect of surface convection and radiation at the interface between active and inactive elements can lead to errors in the elements' activation and proposed methods to minimize mistakes. In the author's work, a new hybrid method of quiet inactive metal deposition was proposed, according to which the elements corresponding to metal deposition are inactive at first and then gradually switch to the quiet method. As a result of this approach, equivalent heat transfer results are achieved, but at the same time, the program operation time is significantly reduced.

One of the significant problems in the SLM process using metal powders is the thermal deformation of the model during moulding. Since the hardened part cools quickly, the model tends to deform and crack due to thermal effects. In the case of the formation of a three-dimensional overhanging model, the overhanging part is destroyed and the construction of the model cannot be completed. Therefore, when constructing products with overhanging parts, it is necessary to make the first sintered layer on the underlying powder non-deformable, since the underlying powders do not limit the movement of subsequent sintered layers. In Ref. [79], a method was proposed for calculating the distribution of temperature and stresses within a single metal layer formed on a powder layer during rapid prototyping by the SLM method. It was assumed that the hardened layer undergoes planar deformation under stress, and two-dimensional finite element methods were combined for thermal conductivity and elastic deformation. In the simulation, a finite element grid was built on the surface of the powder layer. The heat caused by the laser radiation was given to the elements under the laser beam. It was believed that shrinkage because of solidification leads only to a change in the thickness of the layer. In modelling elastic finite elements, Young's modulus of the solidified part was expressed as a function of temperatures. To simplify calculations, the entire area was treated as continuous, and the powder layer and the molten part were considered to have a very small Young's modulus.

Calculations of thermal conductivity and elastic finite elements were performed alternately. The obtained results of deformation and distribution of tensile stresses showed the possibility and places of cracking of the layer during the moulding process. It turned out that the solid layer on the powder layer was deformed due to heating and cooling during the movement of the laser beam along the track. The stress distribution in the hardened part, caused by temperature changes during moulding, showed a striped pattern of compressive and tensile stresses. When the adjacent track solidified, large tensile stresses appeared at the side end of the solid layer between the hardened tracks, which could subsequently lead to cracks.

In Ref. [84], an approach to 3*D* modelling is proposed that allows us to evaluate the interaction of powder with laser and atmosphere in the process of three-dimensional printing using SLM technology. By comparing the numerical and experimental results, a reasonably good correlation was found between the simulated and experimental data on the width and depth of the melt bath. It has been shown that the depth and width of the melt bath are directly proportional to the effective scanning speed of the laser. The size of the melt bath decreases with increasing scanning speed (*i.e.*, decreasing exposure time). The exposure time of the laser beam affects the density of energy transferred to the material and, therefore, is an important factor for ensuring complete melting of the material. Reducing the holding time below a definite limit can lead to an increase in porosity. As noted in Refs. [85–87], the stability of the melt bath determines the integrity and quality of the structure of the finished product, *i.e.*, ensures the absence of non-molten areas.

In Ref. [88], using modelling in the ANSYS environment, an approach was investigated to determine the necessary and sufficient number of supporting structures in the construction process of a 316L stainless steel part that can withstand residual stresses and dissipate heat. To do this, the effect of temperature gradients on the distribution of residual stresses for each layer was studied. It has been shown that expansion of the material (*i.e.*, tensile stresses) during the heating cycle and compression of the material during cooling (*i.e.*, compressive stresses) causes shrinkage and cracks in the layer. After the laser beam leaves this area, the irradiated area cools down and tends to shrink. Shrinkage is partially suppressed due to plastic deformation that develops during heating, which leads to a state of residual tensile stress in the irradiation zone. High tensile stresses (occurring along the direction of the laser scan) can also lead to transverse cracking of the layer. Cracking can be avoided by preheating or using shorter scan paths, which reduce the cooling rate. The mechanism that prevents cracking due to preheating increases the material ductility and the possibility of stress relief due to plastic deformation.

It was proposed to monitor the dynamics of temperature changes and the behaviour of solidification of molten powder to study the phenomenon

of accumulation of residual stress using finite element modelling methods [89]. A comparison of the simulation results with experimental data shows that the developed model can predict the temperature distribution in the laser-powder interaction zone, solidification characteristics, cooling rates, width and depth of the melt bath, and, consequently, trends in changes in residual stresses when changing SLM parameters.

In the study framework [89], block samples were considered, made at the same energy density but using different parameters of laser power and glow time. The paper shows that the temperature gradient between the upper boundary of the melt bath and the area 250 microns below the melt bath is higher for a combination of 200 W power parameters and 120 μs laser exposure time compared with a combination of 150 W power parameters and 160 μs laser exposure time. According to Ref. [90], the tendency to decrease the temperature gradient between the surfaces under consideration should lead to a decrease in residual stress. In addition, the work shows that the highest temperature in the melt bath decreases with a combination of 150 W power parameters and 160 μs laser exposure time compared with a combination of 200 W power parameters and 120 μs laser exposure time. These results are consistent with the conclusions given in Refs. [91, 92], which reports that an increase in laser power has a more pronounced effect on the peak temperature of the melt bath compared with the scanning speed.

Finite element methods were also used in Ref. [93] in conjunction with the computational fluid dynamics software Fluent. As part of the work, a series of scanning strategies were simulated for different numbers of lasers, scan lengths, scan directions, scan directions, and scan sequences. By comparing the simulation results, the effect of scanning strategies on residual stress is studied. The accuracy of the simulation was confirmed by experimental data [89, 94]. Studies have shown that the 'dual-zone technique' (S14C) scanning strategy results in a 10.6% reduction in residual voltage compared to the traditional sequential scanning strategy. The residual voltage is significantly higher when the number of lasers is increased to four, which is associated with an increase in the amount of heat supplied. The residual voltage is sensitive to the scan length for both single-laser and multilaser strategies, but there is no constant correlation between them. When the scanning length decreases in the SLM process with a single laser, the average longitudinal voltage initially increases slightly by 4.6% and then sharply declines by 13.0%. For a multi-laser SLM process, the scanning sequence and the scanning direction are two main factors in controlling residual voltage. After changing the scan sequence, the average equivalent voltage is reduced by 19.0%. Meanwhile, when the direction of movement is changed, the average relevant voltage decreases by 6.2%. The names of the scans S14C, S41A, S41B, S42A, and S42B were introduced by the authors of the work and illustrated in detail in the article [94].

11. The Possibilities of 3*D* Printing to Produce Real Objects

The study of materials and structures made of metals, whose internal structural elements range in size from tens nm to several mm, has been actively underway for many years. The problem, however, is that it has not yet been possible to develop technologies for the mass production of such materials. At the same time, laboratory studies have established that they may have unique properties. For example, they are capable of absorbing light in optically active metamaterials [95] or increasing the ability of a part to resist deformation under mechanical stress [96].

In general, nanoscale objects are obtained in two ways. In the so-called bottom-up approach, an object is created as a result of combining smaller structural units of matter: atoms, molecules, or nanoobjects of smaller size. With the 'top–down' approach, a macroscopic amount of matter is crushed to the nanoscale, or nanoscale pattern patterns are formed in a macroscopic sample.

Metal products with an internal nanostructure are now able to be produced using nanolithography, nanotraveling, and using a laser to form nanoscale parts on the metal surface. These methods are expensive and complex, which limits the possibility of scaling them to industrial volumes. Another disadvantage is that these methods are almost impossible to create a full-fledged internal three-dimensional nanostructure inside a macroscopic metal billet, so they are most often used to make a microrelief (nanoscale rises or depressions) on the surface.

It is assumed that three-dimensional printing (which can be considered as a kind of bottom-up approach) can cope with the creation of metal metamaterials with a complex internal structure: the desired object is lined up layer by layer with a 3*D* printer according to a three-dimensional drawing (therefore, this method is also called 'layered synthesis'). Now, it is already possible to manufacture parts containing nanoscale structural elements that cannot be obtained using traditional top–down methods for obtaining nanoobjects, but, alas, not from metals. Since the beginning of 2010, the 'one-year-old' appeared in technology due to the use of three-dimensional structures made of polymers [97] and ceramics [98].

However, metals have not yet been able to be used for printing with nanometre resolution. At the same time, various methods of three-dimensional printing of reasonably small structures made of metals already exist, but their resolution is 20–50 μm [99]. The resolution of three-dimensional printing is determined by the form, in which the 'ink' (in this case, metal) is fed into the printer, and the effects expose to them during the layered printing process. Thus, in layered synthesis, which most nearly resembles traditional printing on a printer, when metal-containing ink is passed through the printer nozzles, the solidifying droplets have a diameter of 40–60 microns, so the tiny elements of the product structure can-

not be smaller. During plasma deposition, metal wire with a diameter of more than 100 microns is used as a raw material, which melts under the influence of plasma pulses, and the tiniest elements of the parts are obtained in the order of hundreds of micrometres [100]. During laser sintering or melting, metal-powder particles have a size of 0.3–10 μm, and the minimum size of the 'pattern' on the surface of the printed part turns out to be about 20 μm [101].

Since, ultimately, three-dimensional metal printing is an ascending method the printed parts will always be larger than the elements that serve as 'ink' for printing, the size of which will determine the print resolution. It is possible to overcome all these limitations if we develop a fundamentally new scheme of layered synthesis that allows us to work with metal or metal-containing precursors on nanometre scales without any problems.

This was done by Julia R. Greer's group of scientists from the California Institute of Technology. Previously, this group has already developed methods for the three-dimensional printing of nanoscale devices made of polymers and ceramics. The success of the new technology lies in replacing metal powders and wires used in other types of three-dimensional printing with a fundamentally different type of metal source: a metal-containing organic polymer. This polymer is simpler to mould to form nanoscale structures. According to the plan of chemists from California, it was supposed to become a template that promotes the correct metal distribution in the printing product.

To obtain metal-containing inks, nickel (II) acrylate was initially produced, in which the residues of unsaturated acrylic acid retained the ability to polymerise (Fig. 5). The metal-containing monomer was mixed with another acrylic monomer, pentaerythritol triacrylate and 7-diethylamino-2-tenoyl coumarin, which played the role of initiator of the photochemical polymerisation process. Polymer blanks of the desired shape were formed from the resulting mixture using one of the three-dimensional printing methods — two-photon lithography. In that section of the reaction mixture, which was irradiated with a laser, photoactivation of 7-diethylamino-2-tenoyl coumarin took place, due to which the polymer containing chemically bonded nickel atoms solidified.

At the next stage, the blanks made of nickel-containing polymer were pyrolyzed. To do this, they were placed in a vacuum chamber of a muffle furnace and slowly heated to 1000 °C. This temperature is almost 500 °C lower than the melting point of Ni (1455 °C). Still, it turned out to be quite enough to remove the organic component of the polymer, leaving a nanostructure, which, according to the results of research using energy dispersive x-ray spectroscopy, contained 91.8% of Ni. The high temperature also contributed to the unification of the remaining metal atoms into shapes that repeated the original polymer structures but were smaller in size. Since most of the material that made up the metal-polymer structure

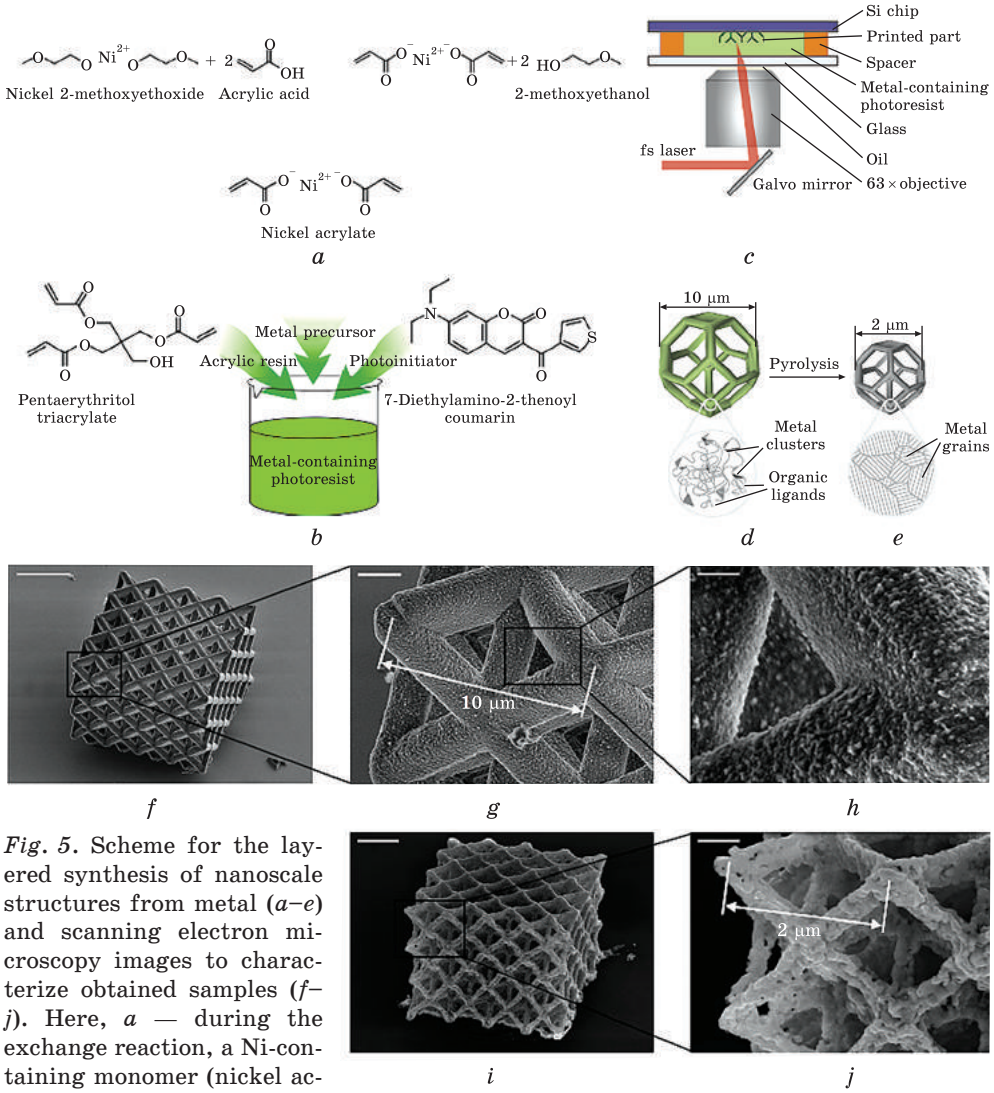

Fig. 5. Scheme for the layered synthesis of nanoscale structures from metal (*a*–*e*) and scanning electron microscopy images to characterize obtained samples (*f*–*j*). Here, *a* — during the exchange reaction, a Ni-containing monomer (nickel acrylate) is obtained, the multiple bonds of acrylic acid residues which are capable of entering into a polymerization reaction; *b* — Ni-containing monomer, acrylic resin (pentaerythritol triacrylate) and the initiator of photochemical polymerization (7-diethylamino-2-tenoyl coumarin) are mixed to obtain transparent Ni-containing 'ink' for 3*D* printing; *c* — schematic representation of the applied approach for 3*D* printing — two-photon lithography; *d* — printed blank made of a Ni-containing polymer and undergoes pyrolysis; *e* — as a result of which the organic component of the polymer is removed and a nanoscale metal structure remains; *f*–*h* — 3*D* mesh printed from a Ni-containing polymer; *i*–*j* — as a result of which almost only one Ni remains in the structure [108]

evaporated during pyrolysis, the metal products obtained after pyrolysis decreased by 80% (Fig. 5). The internal elements of metal parts obtained using the new approach can be characterized by size from hundreds of nanometres to micrometres; even such a resolution in three-dimensional printing of metal structures it was not possible.

Now, researchers are trying to improve the developed methodology. First of all, we need to learn how to eliminate defects in the structure of the resulting metal objects: the article honestly admits that the metal structures obtained after pyrolysis contain voids and differ in an uneven surface (this is clearly visible in Figs. 1 and 3), and include a small amount of impurities, mainly carbon. Since impurities and minor defects can seriously affect electronic and optical properties, these problems must be solved before the industrial use of the new approach.

The researchers also plan to test the approach they have developed for the three-dimensional printing of structures made of other metals. The most interesting in this regard seems to be an attempt to use tungsten, whose high melting point (3442 °C) does not allow the use of traditional metal printing methods.

Despite the significant number of advantages of three-dimensional printing in the layout of objects, the creation of actual details is of greater interest.

Additive manufacturing technologies in the industry have considerable prospects. Small-scale production of products with complex geometric shapes and made of specific materials is widespread in the oil and gas industry, shipbuilding, energy engineering, reconstructive surgery and dental medicine, and the aerospace industry. The direct cultivation of metal products here is motivated by economic expediency since this production method turned out to be less expensive. Using additive technologies, working parts of drive mechanisms and shafts, implants, and endoprostheses, spare parts for cars and aeroplanes are produced. The development of rapid production was also facilitated by the significant expansion of the number of available metal powder materials. If in 2000 there were 5–6 types of powders, now, a wide range is offered, numbering dozens of compositions from structural steels to precious metals and heat-resistant alloys. Additive technologies are also promising in mechanical engineering, where they can be used in the manufacture of tools and devices for mass production — inserts for thermoplastics machines, moulds, and templates [102].

There are three directions in the use of additive technologies in industry: increasing the reliability of equipment, increasing the maintainability of equipment, and manufacturing fundamentally new equipment.

Oil and gas equipment itself is reliable and unpretentious, as it was designed for harsh working conditions, but over time, reliability decreases and no longer reaches the required level. Traditional methods of repair and restoration can return full functionality, but not reliability, therefore, after each subsequent repair, the operating time of the equipment

decreases until a critical moment comes when repair is impractical, and the equipment is scrapped. Premature equipment failure is also affected by an aggressive environment in which the equipment does not produce even 50% of its service life [102].

The use of three-dimensional printing technologies will improve the reliability of the equipment without resorting to constructive interference in the equipment. There are two ways to achieve increased reliability. The first way is the use of materials for the manufacture of equipment parts with improved performance and properties. The second way is to manufacture equipment parts in one array, excluding welding and soldering joints.

Most of the industrial equipment and machines operate in a harsh operating mode. One of the essential components is the conditions that ensure the necessary operation of the equipment. Such conditions include high temperature, overpressure, and extreme mechanical loads. Equipment failure statistics show that equipment failure due to a defect at the junction accounts for up to 18% of all breakdowns. Such defects include burnouts of gaskets and destruction of gaskets and seals due to increased pressure and aggressiveness of the medium. The connection points are the weak link of each piece of equipment [103–106].

12. Conclusions

Additive manufacturing methods are an alternative to existing traditional methods of manufacturing parts. Unlike the subtractive methods of product production, where everything superfluous is cut off from the workpiece, three-dimensional printing methods 'grow' apart from a powder composition, the particles of which are synthesized in each layer and the layers among themselves. The use of additive technologies makes it possible to obtain products with internal cavities of any shape (rectangular, spiral, mesh), for instance, cooling channels for heat exchangers, casting tools for creating new engine housings, and parts with a mesh structure.

Additive technologies provide new opportunities in the manufacturing process of metal parts for mechanical engineering [109–114]. Therefore, three-dimensional printing is an innovative method that allows you to create complex and voluminous metal parts. This article discusses the use of three-dimensional printing in metal product production. The paper describes the basic principles of three-dimensional printing and its advantages and disadvantages. Various types of three-dimensional printing used to create metal products are also considered. We also discussed the main aspects of the application of this method and its impact on the quality and functional properties of manufactured parts. Finally, we analysed the application of additive technologies in the process of manufacturing metal parts.

REFERENCES

1. W.E. King, A.T. Anderson, R.M. Ferencz, N.E. Hodge, C. Kamath, S.A. Khairallah, and A.M. Rubenchik, *Appl. Phys. Rev.*, **2**: 41304 (2015). https://doi.org/10.1063/1.4937809
2. K. Osakada and M. Shiomi, *Int. J. Machine Tools & Manufacture*, **46**: 1188 (2006). https://doi.org/10.1016/j.ijmachtools.2006.01.024
3. I.E. Volokitina, *Met. Sci. Heat Treat.*, **61**, Nos. 3–4: 234 (2019). https://doi.org/10.1007/s11041-019-00406-1
4. X.P. Li, C.W. Kang, H. Huang, L.C. Zhang, and T.B. Sercombe, *Mater. Sci. Eng. A*, **606**: 370 (2014). https://doi.org/https://doi.org/10.1016/j.msea.2014.03.097
5. I.E. Volokitina, A.V. Volokitin, M.A. Latypova, V.V. Chigirinsky, and A.S. Kolesnikov, *Prog. Phys. Met.*, **24**, No. 1: 132 (2023). https://doi.org/10.15407/ufm.24.01.132
6. R. Morgan, C. Sutcliffe, and W. O'Neill, *J. Mater. Sci.*, **39**, No. 4: 1195 (2004).
7. J. Majumdar and I. Manna, *Laser Process. Mater.*, **28**: 495 (2003). https://doi.org/10.1007/BF02706446
8. A. Bychkov and A. Kolesnikov, *Metallogr. Microstruct. Anal.*, **12**, No. 3: 564 (2023). https://doi.org/10.1007/s13632-023-00966-y
9. I.E. Volokitina and A.V. Volokitin, *Metallurgist*, **67**: 232 (2023). https://doi.org/10.1007/s11015-023-01510-7
10. I. Volokitina, B. Sapargaliyeva, A. Agabekova, G. Ulyeva, A. Yerzhanov, and P. Kozlov, *Case Studies Construct. Mater.*, **18**: e02162 (2023). https://doi.org/10.1016/j.cscm.2023.e02162
11. C.Y. Yap, C.K. Chua, Z.L. Dong, Z.H. Liu, D.Q. Zhang, L.E. Loh, and S.L. Sing, *Appl. Phys. Rev.* **2** (2015). https://doi.org/10.1063/1.4935926
12. I.E. Volokitina, A.V. Volokitin, and E.A. Panin, *Prog. Phys. Met.*, **23**, No. 4: 684 (2022). https://doi.org/10.15407/ufm.23.04.684
13. A. Naizabekov, A. Volokitin, and E. Panin, *J. Mater. Eng. Perform.*, **28**, No. 3: 1762(2019). https://doi.org/10.1007/s11665-019-3880-6
14. H.D. Zhao, F. Wang, Y.Y. Li, and W. Xia, J. Mater. Process. Technol., 219: 4537 (2009).
15. A. Denissova, Y. Kuatbay, and Y. Liseitsev, *Case Studies Construct. Mater.*, **19**: e023462023. https://doi.org/10.1016/j.cscm.2023.e02346
16. A.B. Spierings, K. Dawson, K. Kern, F. Palm, and K. Wegener, *Mater. Sci. Eng. A*, **701**: 264 (2017). https://doi.org/10.1016/j.msea.2017.06.089
17. V. Manakari, G. Parande, and M. Gupta, *Metals*, **7**, No. 1: 2 (2017). https://doi.org/10.3390/met7010002
18. K. Wei, M. Gao, Z. Wang, and X. Zeng, *Mater. Sci. Eng. A*, **611**: 212 (2014). https://doi.org/10.1016/j.msea.2014.05.092
19. L. Thijs, F. Verhaeghe, T. Craeghs, and Jean-Pierre Kruth, *Acta Mater.*, **58**, No. 9: 3303 (2010). https://doi.org/10.1016/j.actamat.2010.02.004
20. J.-P. Kruth, G. Levy, F. Klocke, and T.H.C. Childs, *CIRP Annals*, **56**, No. 2: 730 (2007).

21. S. Lezhnev, A. Naizabekov, E. Panin, and I. Volokitina, *Procedia Engineering*, **81**: 15 (2014).
https://doi.org/10.1016/j.proeng.2014.10.180
22. M. Avalle, G. Belingardi, M.P. Cavatorta, and R. Doglione, *Int. J. Fatigue*, **24**: 1 (2002).
23. I. Gibson, D.W. Rosen, and B. Stucker, *Additive Manufacturing Technologies*, **160** (Boston, MA: Springer: 2010), p. 160.
https://doi.org/10.1007/978-1-4419-1120-9_6
24. X. Gong, T. Anderson, and K. Chou, *Proc. ASME/ISCIE Int. Symp. Flexible Automation. American Society of Mechanical Engineers* (June 18–20, 2012, St. Louis, Missouri, USA), p. 507.
https://doi.org/10.1115/ISFA2012-7256
25. J. Milberg and M. Sigl, *Prod. Eng. Res. Devel.*, **2**: 117 (2008).
https://doi.org/10.1007/s11740-008-0088-2
26. L.E. Murr, E. Martinez, S. Gaytan, D. Ramirez, B. Machado, P. Shindo, J. Martinez, F. Medina, J. Wooten, and D. Ciscel, Metall. Mater. Trans. A, 42: 3491 (2011).
27. S. Biamino, A. Penna, U. Ackelid, S. Sabbadini, O. Tassa, P. Fino, M. Pavese, P. Gennaro, and C. Badini, *Intermetallics*, **19**, No. 6: 776 (2011).
28. I. Volokitina, E. Siziakova, R. Fediuk, and A. Kolesnikov, *Materials*, **15**, No. 14: 4930 (2022).
https://doi.org/10.3390/ma15144930
29. A. Antonysamy, J. Meyer, and P. Prangnell, *Mater. Charact.*, **84**: 153 (2013).
https://doi.org/10.1016/j.matchar.2013.07.012
30. Y.-Y. Kim, *Acta Metall. Mater.*, **40**, No. 6: 1121 (1992).
https://doi.org/10.1016/0956-7151(92)90411-7
31. S. Draper, G. Das, I. Locci, J. Whittenberger, B. Lerch, and H. Kestler, *Mater. Sci. Eng. A*, **243**, No. 1: 257 (1998).
32. P. Heinl, C. Kцrner, and R.F. Singer, *Adv. Eng. Mater.*, **10**, No. 9: 882 (2008).
33. I. Volokitina, Metal Sci. Heat Treat., 62: 253 (2020).
https://doi.org/10.1007/s11041-020-00544-x
34. P. Heinl, L. Müller, C. Körner, R.F. Singer, and F.A. Müller, *Acta Biomater.*, **4**, No. 5: 1536 (2008).
https://doi.org/10.1016/j.actbio.2008.03.013
35. P. Thomsen, J. Malmstrцm, L. Emanuelsson, M. Rene, and A. Snis, *J. Biomed. Mater. Res. B*, **90**, No. 1: 35 (2009).
https://doi.org/10.1002/jbm.b.31250
36. G. Chahine, H. Atharifar, P. Smith, and R. Kovacevic, *Int. Solid Freefrom Fabrication Symposium* (Austin, Texas, USA: 2009), p. 631.
37. L.E. Murr, S.M. Gaytan, A. Ceylan, E. Martinez, J.L. Martinez, D.H. Hernandez, B.I. Machado, D.A. Ramirez, F. Medina, S. Collins, and R.B. Wicker, *Acta Mater.*, **58**, No. 5: 1887 (2010).
https://doi.org/10.1016/j.actamat.2009.11.032
38. D. Cormier, O. Harrysson, T. Mahale, and H. West, *Adv. Mater. Sci. Eng.*, 2007: 034737 (2008).
https://doi.org/10.1155/2007/34737
39. S. Lezhnev, A. Naizabekov, A. Volokitin, and I. Volokitina, *Procedia Engineering*, **81**: 1505 (2014).
https://doi.org/10.1016/j.proeng.2014.10.181
40. I.E. Volokitina, J. Chem. *Technology Metallurgy*, **57**: 631 (2022).
41. O. Harrysson, B. Deaton, J. Bardin, H. West, O. Cansizoglu, D. Cormier, and D. Marcellin-Little, *Materials and Processes for Medical Devices Conference* (2006), p. 15.

42. H. Clemens and H. Kestler, *Adv. Eng. Mater.*, **2**: 551 (2000). https://doi.org/10.1002/1527-2648(200009)2:9%3C551::AID-ADEM551%3E3.0.CO;2-U
43. A.V. Volokitin, I.E. Volokitina, and E.A. Panin, *Prog. Phys. Met.*, **23**, No. 3: 411 (2022). https://doi.org/10.15407/ufm.23.03.411
44. N. Zhangabay, I. Baidilla, A. Tagybayev, U. Suleimenov, Z. Kurganbekov, M. Kambarov, A. Kolesnikov, G. Ibraimbayeva, K. Abshenov, I. Volokitina, B. Nsanbayev, Y. Anarbayev, and P. Kozlov, *Case Studies in Construction Materials*, **18**: e02161 (2023). https://doi.org/10.1016/j.cscm.2023.e02161
45. I. Volokitina, A. Volokitin, E. Panin, T. Fedorova, D. Lawrinuk, A. Kolesnikov, A. Yerzhanov, Z. Gelmanova, Y. Liseitsev, *Case Studies Construct. Mater.*, **19**: e02609 (2023). https://doi.org/10.1016/j.cscm.2023.e02609
46. S.M. Gaytan, L.E. Murr, F. Medina, E. Martinez, M.I. Lopez, and R.B. Wicker, *Mater. Technol.*, **24**: 180 (2009). https://doi.org/10.1179/106678509X12475882446133
47. T. Grimm, *Fused Deposition Modeling: A Technology Evaluation* (2002). https://docplayer.net/9035544-Fused-deposition-modeling-a-technology-evaluation.html
48. K. Karami, A. Blok, L. Weber, S.M. Ahmadi, R. Petrov, K. Nikolic, E.V. Borisov, S. Leeflang, C. Ayas, A.A. Zadpoor, M. Mehdipour, E. Reinton, and V.A. Popovich, *Addit. Manuf.*, **36**: 101433 (2020). https://doi.org/10.1016/j.addma.2020.101433
49. L.E. Murr, S.M. Gaytan, F. Medina, E. Martinez, J.L. Martinez, D.H. Hernandez, B.I. Machado, D.A. Ramirez, and R.B. Wicker, *Mater. Sci. Eng. A*, **527**: 1861 (2010). https://doi.org/10.1016/j.msea.2009.11.015
50. I.E. Volokitina and G.G. Kurapov, *Metal Sci. Heat Treat.*, **59**: 786 (2018). https://doi.org/10.1007/s11041-018-0227-0
51. S.N. Lezhnev, I.E. Volokitina, and A.V. Volokitin, *Phys. Metals Metallogr.*, **118**: 1167 (2017). https://doi.org/10.1134/S0031918X17110072
52. M. Too, K. Leong, C. Chua, Z. Du, S.F. Yang, C.M. Cheah, and S.L. Ho, *Int. J. Adv. Manuf. Technol.*, **19**: 217 (2002). https://doi.org/10.1007/s001700200016
53. M. Sigl, S. Lutzmann, and M. Zдh, *Solid Freeform Fabrication Symposium Proceedings* (2006), p. 397.
54. M. Larsson and A. Snis, *Method and Device for Producing Three-Dimensional Objects* (Google Patents: 2008).
55. S. Knippscheer and G. Frommeyer, *Adv. Eng. Mater.*, **1**: 187 (1999). https://doi.org/10.1002/(SICI)1527-2648(199912)1:3/4%3C187::AID-ADEM187%3E3.3.CO;2-6
56. C. Korner, E. Attar, and P. Heinl, *J. Mater. Process. Technol.*, **211**: 978 (2011). https://doi.org/10.1016/j.jmatprotec.2010.12.016
57. H.B. Qi, Y.N. Yan, F. Lin, W. He, and R.J. Zhang, *Proc. Int. Mech. Eng. B. J. Eng.*, **220**: 1845 (2006). https://doi.org/10.1243/09544054JEM438
58. http://www.up-pro.ru/library/innovations/niokr/additive-3d.html
59. W.M. Steen, *Laser Material Processing* (London: Springer: 2003). https://doi.org/10.1007/978-1-4471-3752-8
60. S. Lezhnev and A. Naizabekov, *J. Chem. Technol. Metallurgy*, **52**, No. 4: 626 (2017).

61. S. Lezhnev and T. Koinov, *J. Chem. Technol. Metallurgy*, **49**, No. 6: 621 (2014).
62. S. Lezhnev and E. Panin, *Advanced Materials Research*, **814**: 68–75 (2013).
63. A.V. Volokitin, M.A. Latypova, A.T. Turdaliev, and O.G. Kolesnikova, *Prog. Phys. Met.*, **24**, No. 4: 686 (2023).
https://doi.org/10.15407/ufm.24.04.686
64. A.T. Turdaliev, M.A. Latypova, and E.N. Reshotkina, *Prog. Phys. Met.*, **24**, No. 4: 792 (2023).
https://doi.org/10.15407/ufm.24.04.792
65. https://habr.com/ru/articles/218271/
66. M. Khan and P. Dickens, *Rapid Prototyping J.*, **18**:81 (2012).
https://doi.org/10.1108/13552541211193520
67. D. Zito, A. Carlotto, A. Loggi, P. Sbornicchia, D. Maggian, P. Unterberg, and I. Cristofolini, *Optimization of SLM Technology Main Parameters in the Production of Gold and Platinum Jewelry, Proc. Santa Fe Symposium, Albuquerque* (2014), p. 1.
68. D. Ding, Z. Pan, and D. Cuiuri, *Int. J. Adv. Manuf. Technol.*, **81**: 465 (2015).
https://doi.org/10.1007/s00170-015-7077-3
69. J. Dawes, R. Bowerman, and R. Trepleton, *Matthey Technol. Rev.*, **59**: 243 (2015).
https://doi.org/10.1595/205651315X688686
70. R.M. German, *Powder Metallurgy Science* (Princeton, N.J.: Metal Powder Industries Federation: 1994), p. 167.
71. A.J. Pinkerton and L. Li, *J. Adv. Manuf. Technol.*, **25**: 471 (2005).
https://doi.org/10.1007/s00170-003-1844-2
72. R.J. Herbert, *J. Mater. Sci.*, **51**: 1165 (2016).
https://doi.org/10.1007/s10853-015-9479-x
73. G. Zhu, A. Zhang, D. Li, Y. Tang, Z. Tong, and Q. Lu, *Int. J. Adv. Manuf. Technol.*, **55**: 945 (2011).
https://doi.org/10.1007 /S00170-010-3142-0
74. R. Jendrzejewski, G. Śliwiński, M. Krawczuk, and W. Ostachowicz, *Comput. Struct.*, **82**: 653 (2004).
https://doi.org/10.1016/j.compstruc.2003.11.005
75. R. Jendrzejewski and G. Śliwiński, *Appl. Surf. Sci.*, **254**: 921 (2007).
https://doi.org/10.1016/j.apsusc.2007.08.014
76. R. Ye, J.E. Smugeresky, B. Zheng, Y. Zhou, and E.J. Lavernia, *Mater. Sci. Eng. A*, **428**: 47 (2006).
https://doi.org/10.1016/J.MSEA.2006.04.079
77. P. Peyre, P. Aubry, R. Fabbro, R. Neveu, and A. Longuet, *J. Phys. D: Appl. Phys.*, **41**: 025403 (2008).
https://doi.org/10.1088/0022-3727/41/2/025403
78. A. Lundback and L.E. Lindgren, *Finite Elem. Anal. Des.*, **47**: 1169 (2011).
https://doi.org/10.1016/j.finel.2011.05.005
79. M. Matsumoto, M. Shiomi, K. Osakada, and F. Abe, *Int. J. Mach. Tools Manuf.*, **42**: 61 (2002).
https://doi.org/10.1016/S0890-6955(01)00093-1
80. P. Michaleris, *Finite Elem Anal Des.*, **86**: 51 (2014).
https://doi.org/10.1016/j.finel.2014.04.003
81. Z. Fan and F. Liou, *Titanium Alloys—Towards Achieving Enhanced Properties for Diversified Applications* (Ed. A.K.M. Nurul Amin) (IntechOpen: 2012), ch. 1.
https://doi.org/10.5772/34848
82. L.E. Lindgren and P. Michaleris, *Handbook on Residual Stress (Ed. J. Lu)* (USA: SEM: 2005), vol. 2, p. 47.

83. L.E. Lindgren, H. Runnemalm, and M.O. Nasstrom, I*nt. J. Numer. Methods Eng.*, **44**: 1301 (1999).
https://doi.org/10.1002/(SICI)1097-0207(19990330)44:9%3C1301::AID-NME479%3E3.0.CO;2-K
84. A. Masmoudi, R. Bolot, and C. Coddet, *J. Mater. Process. Technol.*, **225**: 122 (2015).
https://doi.org/10.1016/j.jmatprotec.2015.05.008
85. I.E. Volokitina, *Metal Sci. Heat Treat.*, **63**: 163 (2021).
https://doi.org/10.1007/s11041-021-00664-y
86. I. Volokitina, B. Sapargaliyeva, A. Agabekova, S. Syrlybekkyzy, A. Volokitin, L. Nurshakhanova, F. Nurbaeva, A. Kolesnikov, G. Sabyrbayeva, A. Izbassar, O. Kolesnikova, Y. Liseitsev, and S. Vavrenyuk, *Case Studies Construct. Mater.*, **19**: e02256 (2023).
https://doi.org/10.1016/j.cscm.2023.e02256
87. I.E. Volokitina, *Prog. Phys. Met.*, **3**, No. 24: 593 (2023).
https://doi.org/10.15407/ufm.24.03.593
88. A. Hussein, L. Ha, C. Yan, and R. Everson, *Mater. Design*, **52**: 638 (2013).
https://doi.org/10.1016/j.matdes.2013.05.070
89. H. Ali, H. Ghadbeigi, and K. Mumtaz, *Int. J. Adv. Manuf. Technol.*, **97**: 2621 (2018). https://doi.org/10.1007/s00170-018-2104-9
90. Y. Shi, H. Shen, Z. Yao, and J. Hu, *Opt. Laser Technol.*, **39**: 858 (2007).
https://doi.org/10.1016/j.finel.2014.04.003
91. I. Yadroitsev, P. Krakhmalev, and I. Yadroitsava, *J. Alloys Compd.*, **583**: 404 (2014).
https://doi.org/10.1016/j.jallcom.2013.08.183
92. M. Alimardani, E. Toyserkani, J.P. Huissoon, and C.P. Paul, *Opt. Lasers Eng.*, **47**: 1160 (2009).
https://doi.org/10.1016/j.optlaseng.2009.06.010
93. S. Zou, H. Xiao, F. Ye, Z. Li, W. Tang, F. Zhu, and C. Zhu, *Results Phys.*, **16**: 103005 (2020).
https://doi.org/10.1016/j.rinp.2020.103005
94. M. Masoomi, S.M. Thompson, and N. Shamsaei, *Int. J. Machine Tools Manuf.*, **118**: 73 (2017).
https://doi.org/10.1016/j.ijmachtools.2017.04.007
95. C.F. Guo, T.i Sun, F. Cao, Q. Liu, and Z. Ren, *Light Sci. Appl.*, **3**: e161 (2014).
https://doi.org/10.1038/lsa.2014.42
96. R. Maaß, S. Van Petegem, D. Ma, J. Zimmermann, Daniel Grolimund, F. Roters, H. Van Swygenhoven, and D. Raabe, *Acta Mater.*, **57**: 5996 (2009).
https://doi.org/10.1016/j.actamat.2009.08.024
97. F. Melchels, M. Domingos, T. Klein, J. Malda, P. Bártolo, and D. Hutmacher, *Prog. Polymer Sci.*, **37**, No. 8: 1079 (2012).
https://doi.org/10.1016/j.progpolymsci.2011.11.007
98. A. Zocca, P. Colombo, C. Gomes, and J. Günster, *J. Am. Ceram. Soc.*, **98**: 638 (2015).
https://doi.org/10.1111/jace.13700
99. L. Hirt, A. Reiser, R. Spolenak, and T. Zambelli, *Adv. Mater.*, **29**: 1604211 (2017)
https://doi.org/10.1002/adma.201604211
100. F. Martinaa, J. Mehnen, S.W. Williams, P. Colegrove, and F. Wang, *J. Mater. Process. Technol.*, **212**: 1377 (2012).
https://doi.org/10.1016/j.jmatprotec.2012.02.002
101. M. Vaezi, H. Seitz, and S. Yang, *Int. J. Adv. Manuf. Technol.*, **67**: 1721 (2013).
https://doi.org/10.1007/s00170-012-4605-2

102. ISO/ASTM52900-15, *Standard Terminology for Additive Manufacturing – General Principles – Terminology* (West Conshohocken, PA: ASTM International: 2015).
103. G. Kurapov, E. Orlova, and A. Turdaliev, *J. Chem. Technol. Metall.*, **51**: 451 (2016).
104. A.B. Naizabekov, S.N. Lezhnev, and I.E. Volokitina, *Metal Sci. Heat Treat.*, **57**: 254 (2015).
https://doi.org/10.1007/s11041-015-9870-x
105. I. Volokitina, A. Volokitin, and D. Kuis, J. *Chem. Technol. Metall.*, **56**: 643 (2021).
106. D.A. Sinitsin, A.E.M.M. Elrefaei, A.O. Glazachev, E.I. Kayumova, and I.V. Nedoseko, *Construction Materials and Products*, **6**: 2 (2023).
https://doi.org/10.58224/2618-7183-2023-6-6-2
107. M. Galati and L. Iuliano, *Addit. Manuf.*, **19**: 1 (2018).
https://doi.org/10.1016/j.addma.2017.11.001
108. A. Vyatskikh, S. Delalande, A. Kudo, X. Zhang, C.M. Portela, and J.R. Greer, *Nature Commun.*, **9**: 593 (2018).
https://doi.org/10.1038/s41467-018-03071-9
109. P.E. Markovsky, D.V. Kovalchuk, S.V. Akhonin, S.L. Schwab, D.G. Savvakin, O.O. Stasiuk, D.V. Oryshych, D.V. Vedel, M.A. Skoryk, and V.P. Tkachuk, *Prog. Phys. Met.*, **24**, No. 4: 715 (2023).
https://doi.org/10.15407/ufm.24.04.715
110. P.E. Markovsky, D.V. Kovalchuk, J. Janiszewski, B. Fikus, D.G. Savvakin, O.O. Stasiuk, D.V. Oryshych, M.A. Skoryk, V.I. Nevmerzhytskyi, and V.I. Bondarchuk, *Prog. Phys. Met.*, **24**, No. 4: 741 (2023).
https://doi.org/10.15407/ufm.24.04.741
111. A.V. Zavdoveev, T. Baudin, D.G. Mohan, D.L. Pakula, D.V. Vedel, and M.A. Skoryk, *Prog. Phys. Met.*, **24**, No. 3: 561 (2023).
https://doi.org/10.15407/ufm.24.03.561
112. O.M. Ivasishin, D.V. Kovalchuk, P.E. Markovsky, D.G. Savvakin, O.O. Stasiuk, V.I. Bondarchuk, D.V. Oryshych, S.G. Sedov, and V.A. Golub, *Prog. Phys. Met.*, **24**, No. 1: 75 (2023).
https://doi.org/10.15407/ufm.24.01.075
113. M.O. Vasylyev, B.M. Mordyuk, and S.M. Voloshko, *Prog. Phys. Met.*, **24**, No. 1: 5 (2023).
https://doi.org/10.15407/ufm.24.01.005
114. M.O. Vasylyev, B.M. Mordyuk, and S.M. Voloshko, *Prog. Phys. Met.*, **24**, No. 1: 38 (2023).
https://doi.org/10.15407/ufm.24.01.038

Received 01.02.2024
Final version 26.04.2024

М.А. Латипова[1], *А.Т. Турдалієв*[2]
[1]Карагандинський індустріальний університет,
просп. Республіки, 30, 101400 Темиртау, Казахстан
[2]Південно-Казахстанський університет ім. М. Ауезова,
просп. Тауке хана, 5,
160012 Шимкент, Казахстан

АДИТИВНІ ТЕХНОЛОГІЇ 3*D*-ДРУКУ МЕТАЛАМИ

Адитивні технології 3*D*-друку, що динамічно розвиваються швидкими темпами, використовуються у прогресивних виробництвах. Є кілька видів адитивних технологій, заснованих на різних фізичних принципах: селективне лазерне плавлення, електронно-променеве плавлення, моделювання методом пошарового натоплення, пошарове ламінування тощо. Усіх їх об'єднано одним технологічним принципом — одержанням виробів методом пошарової побудови. Як і традиційні технології формування виробів, кожен із типів адитивних технологій має свої переваги та недоліки. Основними матеріалами, з яких традиційно одержують функціональні вироби різного призначення, є метали та сплави. Нині у світі для виробництва виробів із металів найбільш відпрацьовано дві основні технології: селективне лазерне й електронно-променеве плавлення. Попри високу точність і непогану якість одержуваних виробів ці технології мають низку недоліків, зокрема високу вартість як самого технологічного обладнання, так і сировинних матеріалів.

Ключові слова: селективне лазерне плавлення, адитивні технології, мікроструктура, керування мікроструктурою, термічне оброблення.